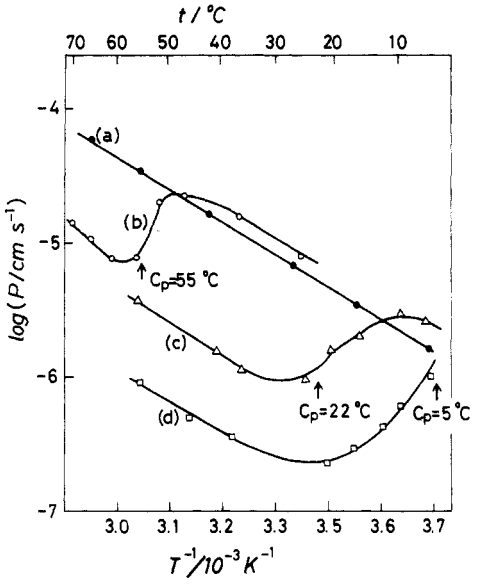

Figure 3. Arrhenius plots of permeation of naphthalenedisulfonate from polymer-grafted capsules: (a) ungrafted capsule; (b) poly(*N*-acryloylpyrrolidine)-grafted capsule (C_p = 55 °C); (c) poly(*N*-*n*-propylacrylamide)-grafted capsule (C_p = 22 °C); (d) poly(*N*-acryloylpiperidine)-grafted capsule (C_p = 5 °C).

Chart I

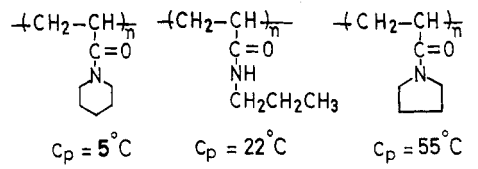

the permeants. Thus, the permeability of the large naphthalenedisulfonate was decreased 12–15 times above C_p = 35 °C relative to that below C_p and 100 times lower than that of the ungrafted capsule. This thermosensitive permeation is reversible: the permeability of naphthalenedisulfonate can be changed repeatedly in the range of 12 within 30 s when the temperature of the outer medium is changed between 25 and 40 °C. Although the permeation of relatively small molecules such as NaCl and benzenesulfonate was decreased to some extent near 35 °C, it was gradually increased as the temperature was raised beyond C_p. Thus, the entangled, corked polymer moves thermodynamically at high temperatures and the permeation of small molecules is hardly suppressed at temperatures beyond C_p.

The temperature region of the thermosensitive permeation of the polymer-grafted capsule can be selected when the poly(*N*-alkylacrylamides) in Chart I having C_p at 5, 22, and 55 °C are employed as grafting polymers. Arrhenius plots of the permeation of naphthalenedisulfonate from polymer-grafted capsules are shown in Figure 3. The permeability decreased at temperatures beyond the corresponding C_p compared with that of the ungrafted capsule.

In conclusion, although nylon capsule membranes are simply semipermeable in proportion to temperature, the poly(*N*-alkylacrylamide)-grafted capsule membrane can reversibly regulate permeability by temperature changes depending on the molecular size of the permeants, in which the grafted polymer acts as a reversible thermovalve. The valve of the grafted polymer can also be opened or shut by pH changes[6] or redox reactions[12] when polyelectrolytes or viologen-containing polymers were employed for a permeation valve, respectively.

Acknowledgment. We are grateful to Dr. Hiroshi Ito (Mitsui Toatsu Chemicals Inc., Japan) for the *N*-alkylacrylamide monomers and to Dr. Shoji Ito (Institute of Polymers and Textiles, Japan) for helpful discussion.

References and Notes

(1) Functional Capsule Membranes. 23.
(2) For part 22, see: Okahata, Y.; Hachiya, S.; Ariga, K.; Seki, T. *J. Am. Chem. Soc.*, in press.
(3) Kondo, T., Ed. "Microencapsulation: New Techniques and Applications"; Techno Inc.: Japan, 1979.
(4) Chang, T. M. S. "Artificial Cells"; Charles C. Thomas Publisher: Springfield, IL, 1972.
(5) Okahata, Y.; Lim, H.-J.; Nakamura, G.; Hachiya, S. *J. Am. Chem. Soc.* **1983**, *105*, 4855. Okahata, Y.; Lim, H.-J. *Ibid.* **1984**, *106*, 4696. Okahata, Y.; Seki, T. *Ibid.* **1984**, *106*, 8065.
(6) Okahata, Y.; Ozaki, K.; Seki, T. *J. Chem. Soc., Chem. Commun.* **1984**, 519.
(7) Okahata, Y.; Ariga, K.; Seki, T. *J. Chem. Soc., Chem. Commun.* **1985**, 920.
(8) Heskins, M.; Guillet, J. E. *J. Macromol. Sci., Chem.* **1968**, *A2*, 1441.
(9) Chiantore, O.; Guaita, M.; Trossarelli, L. *Makromol. Chem.* **1979**, *180*, 969.
(10) Ito, S.; Mizoguchi, K.; Suda, M. *Rep. Res. Inst. Polym. Text. Jpn.* **1984**, *144*, 7.
(11) Ito, H.; Kamio, H.; Nitta, A.; Nakagawa, T. *Polym. Prepr., Jpn.* **1984**, *33*, 615.
(12) Okahata, Y.; Ariga, K.; Seki, T. *J. Chem. Soc., Chem. Commun.*, in press.

Yoshio Okahata,* Hiroshi Noguchi, and Takahiro Seki
Department of Polymer Chemistry
Tokyo Institute of Technology
Ookayama, Meguro-ku, Tokyo 152, Japan
Received September 11, 1985

Highly Selective Transport of Molecular Oxygen in a Polymer Containing a Cobalt Porphyrin Complex as a Fixed Carrier

We describe herein the preparation of a polymer membrane containing [$\alpha,\alpha',\alpha'',\alpha'''$-*meso*-tetrakis(*o*-pivalamidophenyl)porphinato]cobalt(II) 1-methylimidazole (CoPIm) complex (1) through which molecular oxygen permeates with high selectivity ($P_{O_2}/P_{N_2} > 10$) and discuss the transport mechanism of the penetrant in the membrane containing the fixed carrier.

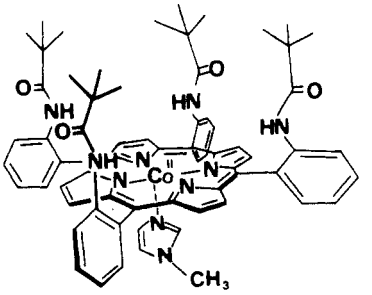

1

Metal complexes such as iron–porphyrin derivatives and cobalt–Schiff base complexes form oxygen adducts reversibly and have been successfully applied to an oxygen-transporting fluid[1] and to an oxygen-separating liquid membrane.[2] These metal complexes bind oxygen according to a Langmuir isotherm. A polymer membrane containing the metal complex as a fixed carrier is expected to sorb and transport oxygen selectively by the Langmuir mode. From this viewpoint, a polymer membrane was

0024-9297/86/2219-0494$01.50/0

Table I
Oxygen Permeability Coefficient (at 25 °C) and Permeability Ratio (P_{O_2}/P_{N_2})

CoPIm in membrane, wt %	permeability coeff[a]	P_{O_2}/P_{N_2}
0	6.4	3.2
2.5	9.8	4.8
4.5	23	12

[a] Upstream pressure: 5.0 mmHg. The permeability coefficient is expressed in units of $(cm^3\ (STP)\cdot cm)/(cm^2\cdot s\cdot cmHg) \times 10^{10}$.

prepared by homogeneously dispersing in poly(butyl methacrylate) the CoPIm complex, whose sixth coordination site is vacant even in the solid state to bind oxygen rapidly and reversibly,[1,3] and the permeability of oxygen and nitrogen (P_{O_2}, P_{N_2}) in the membrane was measured.

A toluene solution of poly(butyl methacrylate) and CoPIm was carefully cast on a Teflon plate under an atmosphere without oxygen, followed by drying in vacuo, to yield a transparent and wine red membrane. Reversible oxygen binding to the CoPIm complex in the membrane in response to a partial pressure of oxygen was observed with spectral change in the visible absorption (λ_{max} 527 nm (deoxy), λ_{max} 545 nm (oxy:O_2/Co = 1/1 adduct), with isosbestic points at 480, 537, and 667 nm). This change occurred very rapidly; e.g., for a 20-μm-thick membrane containing 2.5 wt % CoPIm the oxygen binding/dissociation equilibrium for CoPIm was established within a few minutes after exposure to oxygen ($p_2(O_2)$ = 760 mmHg) or in vacuo at 25 °C. The oxygen-binding equilibrium constant ($K = k_{on}/k_{off}$) was determined to be 5.61×10^{-3} $mmHg^{-1}$ at 25 °C by measuring the oxygen binding/dissociation equilibrium curve by using Drago's equation.[4]

$$\text{CoPIm} + O_2 \underset{k_{off}}{\overset{k_{on}}{\rightleftharpoons}} O_2\text{–CoPIm}$$

Rapid and reversible oxygen binding to the CoPIm complex in the membrane was also confirmed by flash photolysis (using a pulse and laser flash spectrophotometer equipped with a kinetic data processor). Photodissociation of the bound oxygen from CoPIm in the membrane was successfully observed, which gave apparent oxygen binding and dissociation rate constants ($k'_{on} = 5.2 \times 10^5$ $L\cdot mol^{-1}\cdot s^{-1}$, $k'_{off} = 2.7 \times 10^2$ s^{-1}). One of the advantages of this membrane is that ad- and desorption rate and equilibrium constants of the penetrant to the carrier site can be evaluated in situ.

The permeability ratio (P_{O_2}/P_{N_2}) was measured with a low-vacuum permeation apparatus and is given in Table I. The ratio was above 10 for the membrane containing 4.5 wt % CoPIm.

Figure 1 shows the effect of upstream gas pressure (p_2) on P_{O_2} and P_{N_2}. Although the dependence of P on p_2 has been often reported for glassy polymers,[5] glass transition temperatures were 19, 15, and 20 °C for the membranes containing 0, 2.5, and 4.5 wt % CoPIm, respectively, and the membranes were in a rubber state at the temperature for the permeability measurement (25 °C). In fact P_{N_2} is independent of $p_2(N_2)$ as shown in Figure 1. P_{O_2} increases with decreasing $p_2(O_2)$, which suggests that oxygen transport occurs by dual-mode transport (Henry mode and additive Langmuir mode). That is, P is equal to the sum of a first term representing the Henry mode and a second term for the Langmuir mode, which is a function of p_2.[6,7]

$$P = k_D D_D + D_C C K/(1 + K p_2) \quad (1)$$

Here, P is the permeability coefficient, k_D is the solubility coefficient for Henry's law, D_D and D_C are the diffusion coefficients for Henry-type and Langmuir-type diffusion,

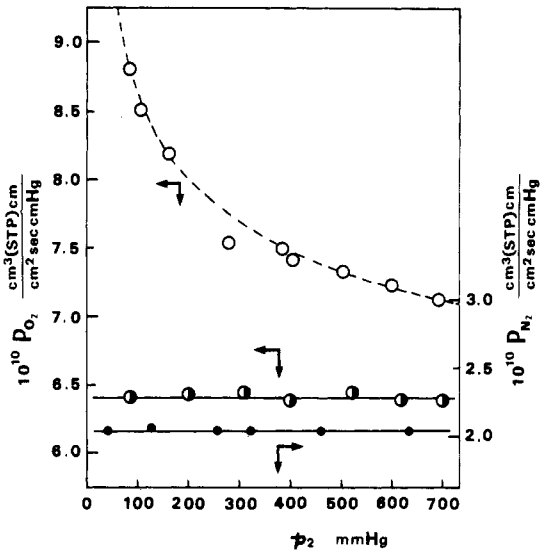

Figure 1. Effect of upstream pressure (p_2) on oxygen (○) and nitrogen (●) permeability in the membrane containing the 2.5 wt % CoPIm complex and on oxygen permeability (◑) in the membrane without CoPIm.

C is the saturated amount of oxygen reversibly bound to the binding site or fixed carrier, K is the oxygen binding/dissociation equilibrium constant, and p_2 is the upstream gas pressure.

The K value mentioned above, C (4.1×10^{-1} cm^3 $(STP)\cdot cm^{-3}$) calculated from the CoPIm concentration in the membrane, D_D (4.3×10^{-7} $cm^2\cdot s^{-1}$) and k_D (1.5×10^{-3} cm^3 $(STP)\cdot cm^{-3}\cdot cmHg^{-1}$) determined by measuring the permeability at 25 °C for the membrane containing the corresponding inert $Co^{III}PIm$ complex (unable to bind oxygen), and an appropriate D_C value (1.5×10^{-8} $cm^2\cdot s^{-1}$) are substituted in eq 1; the calculated curve of P_{O_2} vs. $p_2(O_2)$ is shown as the dashed line in Figure 1. The experimental plots agree with the dashed line, which supports dual-mode transport of oxygen in the membrane and a pathway of oxygen permeation via the fixed carrier.

Although dual-mode transport due to partial immobilization[6] has been reported for carbon dioxide permeation in glassy polymers,[5-7] we herein have verified the dual-mode transport by using a simpler system and have shown the possibility of high permselectivity with a membrane containing a fixed carrier.

Acknowledgment. This work was partially supported by a Grant-in-Aid from the Ministry of Education, Science and Culture, Japan, and the Asahi Glass Foundation for Industrial Technology.

Registry No. CoPIm, 53675-32-4; poly(butyl methacrylate) (homopolymer), 9003-63-8; oxygen, 7782-44-7.

References and Notes

(1) (a) Tsuchida, E. *J. Macromol. Sci., Chem.* **1979**, *A13*, 545. (b) Tsuchida, E.; Nishide, H.; Yuasa, M.; Hasegawa, E.; Matsushita, Y.; Eshima, K. *J. Chem. Soc., Dalton Trans.* **1985**, 275. (c) Tsuchida, E. *Ann. N.Y. Acad. Sci.* **1985**, *446*, 429. (d) *Chem. Eng. News* Jan 14, 1985, 42.
(2) Roman, I. C.; Baker, R. W. Eur. Patent 0098731, 1983 (to Bend Research Co.).
(3) Collman, J. P.; Brauman, J. I.; Coxsee, K. M.; Halbert, T. R.; Hayes, S. E.; Suslick, K. S. *J. Am. Chem. Soc.* **1978**, *100*, 2761.
(4) Beugelsdijk, T. J.; Drago, R. S. *J. Am. Chem. Soc.* **1975**, *97*, 6466.
(5) (a) Koros, W. J.; Paul, D. R.; Rocha, A. A. *J. Polym. Sci., Polym. Phys. Ed.* **1976**, *14*, 687. (b) Koros, W. J.; Paul, D. R. *J. Polym. Sci., Polym. Phys. Ed.* **1978**, *16*, 2171.
(6) Paul, D. R.; Koros, W. J. *J. Polym. Sci., Polym. Phys. Ed.* **1976**, *14*, 675.

(7) Paul, D. R. *Ber. Bunsenges. Phys. Chem.* **1979**, *83*, 294.

Hiroyuki Nishide, Manshi Ohyanagi, Osamu Okada, and Eishun Tsuchida*

Department of Polymer Chemistry
Waseda University, Tokyo 160, Japan

Received October 11, 1985

Long-Range Conformational Structure and Low-Frequency Isotropic Raman Spectra of Some Highly Disordered Chain Molecules

We report here measurements on a unique Raman band whose position and shape are directly related to statistical averages associated with the conformation of highly disordered chain molecules. The band of interest, the "D-LAM" band, has previously been identified only in the low-frequency isotropic Raman spectra of polyethylene[1,2] and poly(tetrafluoroethylene).[1] The aim of the present work is to demonstrate that D-LAM bands exist in the Raman spectra of other kinds of polymers. Measurements on some simple chain molecules in the amorphous and liquid states are presented and, in all cases, D-LAM bands are found.

It is possible, at least in principle, to relate parameters associated with the D-LAM band, in particular its frequency and half-width, directly to certain conformational statistics. The band itself is highly inhomogeneous, being comprised of a complex of bands representing delocalized skeletal-bending modes. Its intensity is attributable to the LAM-like "in-phase", or "breathing" character of the contributing modes, and for this reason the resulting complex is referred to as the "D-LAM band", where LAM is an acronym for longitudinal acoustic mode and D stands for disorder. Because the band has a low depolarization ratio, it can be distinguished from nearly all other kinds of bands in the low-frequency Raman spectrum. Although D-LAM is intrinsically inhomogeneous, it behaves in some ways like a homogeneous band. For example, its frequency depends in a simple way on the number, n, of skeletal atoms in the chain; i.e., its frequency is proportional to $1/n^2$, and depends on the average conformation of the chain.[1] The bandwidth is determined by the dispersion about the average conformation. Both the peak frequency and bandwidth have been shown to increase with the number of gauche bonds in the case of poly(methylene)-type chains.[1] These relations have been used to advantage to characterize the highly disordered, amorphous component in semicrystalline polyethylene.[2]

The chain molecules for which new Raman data are presented here are listed in Table I along with polyethylene and poly(tetrafluoroethylene). The Raman spectra, which are shown in Figures 1–3, were measured with an ISA Ramanor U-100 spectrometer system. The measurements were made with a right-angle scattering geometry, with 300–350 mW of the argon ion 5145-Å line, and with a resolution of 2–3 cm^{-1}. The isotropic spectra were obtained in the usual manner by subtracting the perpendicular spectrum from the parallel spectrum, i.e., $I_{iso} = I_{\parallel} - sI_{\perp}$, where the parameter s was adjusted to eliminate depolarized bands. Depending on experimental conditions, s had a value between 1.18 and 1.75.

For the polymers we studied, the D-LAM band appears below 300 cm^{-1} and is the prominent feature in all the isotropic Raman spectra shown in Figures 1–3. Its shape tends to be symmetric, but there are a number of complicating spectral features. A more complete and quantitative interpretation of these spectra will be reported later. Here we will briefly discuss some of the more ap-

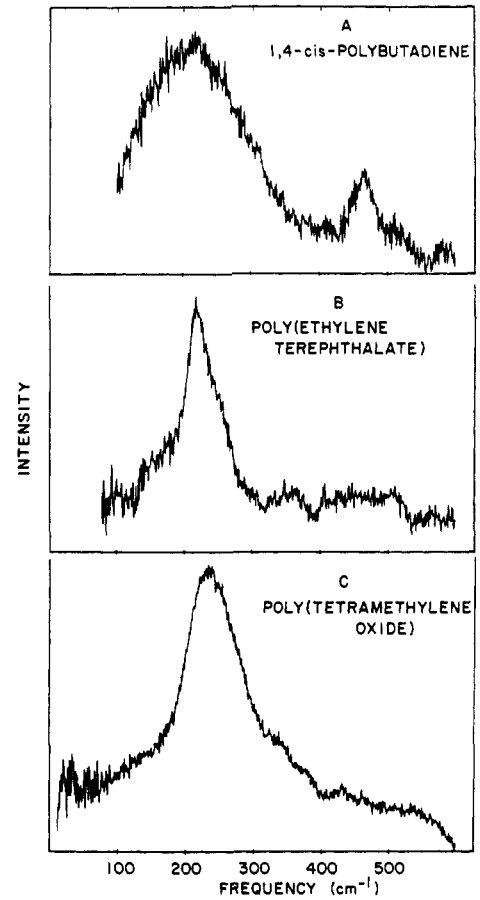

Figure 1. Low-frequency isotropic Raman spectra of liquid (A) 1,4-*cis*-polybutadiene, (B) poly(ethylene terephthalate), and (C) poly(tetramethylene oxide).

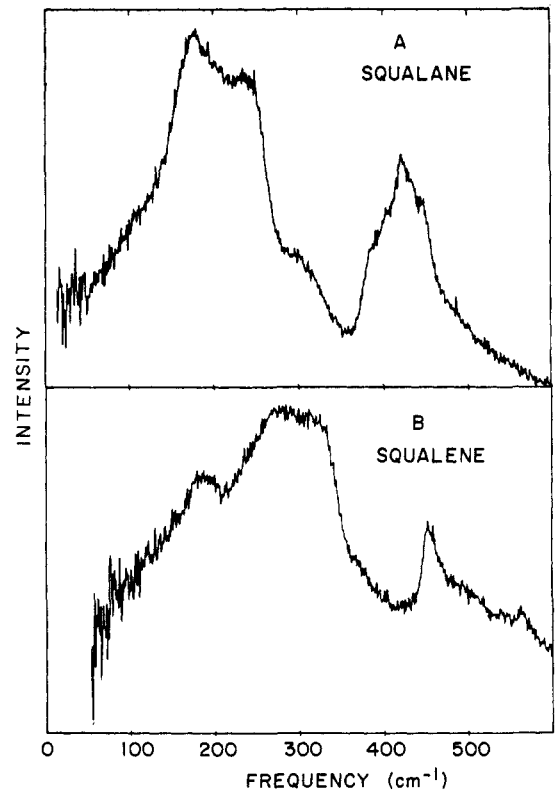

Figure 2. Low-frequency isotropic Raman spectra of liquid (A) squalane and (B) squalene.

0024-9297/86/2219-0496$01.50/0